Published OnlineFirst July 6, 2011; DOI:10.1158/0008-5472.CAN-11-1431

Molecular and Cellular Pathobiology

Cancer Research

Dual Function of ERRα in Breast Cancer and Bone Metastasis Formation: Implication of VEGF and Osteoprotegerin

Anaïs Fradet[1,2], Helène Sorel[1,2], Lamia Bouazza[1,2], Delphine Goehrig[1,2], Baptiste Dépalle[1,2], Akeila Bellahcène[4], Vincent Castronovo[4], Hélène Follet[1,2], Françoise Descotes[3], Jane E. Aubin[5], Philippe Clézardin[1,2], and Edith Bonnelye[1,2]

Abstract

Bone metastasis is a complication occurring in up to 70% of advanced breast cancer patients. The estrogen receptor-related receptor alpha (ERRα) has been implicated in breast cancer and bone development, prompting us to examine whether ERRα may function in promoting the osteolytic growth of breast cancer cells in bone. In a mouse xenograft model of metastatic human breast cancer, overexpression of wild-type ERRα reduced metastasis, whereas overexpression of a dominant negative mutant promoted metastasis. Osteoclasts were directly affected and ERRα upregulated the osteoclastogenesis inhibitor, osteoprotegerin (OPG), providing a direct mechanistic basis for understanding how ERRα reduced breast cancer cell growth in bone. In contrast, ERRα overexpression increased breast cancer cell growth in the mammary gland. ERRα-overexpressing primary tumors were highly vascularized, consistent with an observed upregulation of angiogenic growth factor, the VEGF. In support of these findings, we documented that elevated expression of ERRα mRNA in breast carcinomas was associated with high expression of OPG and VEGF and with disease progression. In conclusion, our results show that ERRα plays a dual role in breast cancer progression in promoting the local growth of tumor cells, but decreasing metastatic growth of osteolytic lesions in bone. *Cancer Res; 71(17); 5728–38. ©2011 AACR.*

Introduction

Bone metastasis is a frequent complication of cancer, occurring in up to 70% of patients with advanced breast cancer. Bone metastasis is not a direct cause of death but is associated with significant morbidity (1). For cancer cells to grow in bone, malignant cells recruit and activate osteoclasts (OC; bone resorbing cells) to resorb the bone matrix. Indeed, osteolytic breast cancer metastasis are characterized by an increase in OC number and activity at the bone metastatic site, where excessive bone destruction provides a permissive microenvironment for breast cancer cells to proliferate and expand (2, 3). Unfortunately, current treatments for bone metastasis that rely on antiresorptive agents are only palliative, raising the need for a better understanding of the molecular mechanisms involved in this pathology so as to design potential alternative therapies (3, 4).

Nuclear steroid receptors are transcription factors that comprise both ligand-dependent molecules such as estrogen receptors (ER) and a large number of so-called orphan receptors, for which no ligand has yet been determined (5). Three orphan receptors, estrogen receptor-related receptor alpha (ERRα), ERRβ, and ERRγ, share structural similarities with ERα and ERβ (5), but they do not bind estrogen (6, 7). Sequence alignment of ERRα and the ERs reveals a high similarity (68%) in the 66 amino acids of the DNA binding domain, but only a moderate similarity (36%) in the ligand-binding domain, which may explain the fact that ERRα recognizes the same DNA binding elements as ERs but does not bind estrogen (8). Although ERRα activity is decreased by the synthetic molecule XCT790, no natural ligand has yet been found (9–11).

ERRα is known to regulate fatty acid oxidation and the adaptive bioenergetic response (12, 13). It is widely expressed in normal tissues, but several RNA expression studies show its presence in a range of cancerous cells including breast, prostate, endometrial, colorectal, and ovarian tumor tissues (14–20). ERRα was markedly increased in neoplastic versus normal tissues, and ERRα-positive tumors were associated with more invasive disease and higher risk of recurrences (14, 15). On the contrary, ERα and ERβ were significantly lower in neoplastic versus normal tissue and were associated with better prognosis (14, 17, 18). ERRα is also highly expressed in skeletal tissues (21, 22) and has been reported to regulate

Authors' Affiliations: [1]Inserm, UMR1033; [2]University of Lyon; [3]Centre hospitalier Lyon Sud, Lyon, France; [4]University of Liège, Liège, Belgique; and [5]University of Toronto, Toronto, Canada

Note: Supplementary data for this article are available at Cancer Research Online (http://cancerres.aacrjournals.org/).

Corresponding Author: Edith Bonnelye, INSERM, UMR1033, UFR de Médecine Lyon-Est, Rue G Paradin 69372 Lyon cedex 08, France. Phone: 33-4-787-857-38; Fax: 33-4-787-787-72; E-mail: edith.bonnelye@inserm.fr

doi: 10.1158/0008-5472.CAN-11-1431

Published OnlineFirst July 6, 2011; DOI:10.1158/0008-5472.CAN-11-1431

osteoblast, OC differentiation, and bone formation *in vitro* (21, 22, 23, 24) and *in vivo* (25–27). Consistent with these observations, osteopontin (OPN) has been reported to be a direct target gene of ERRα in osteoblastic cell lines (28–30). The role of ERRα in bone metastasis formation is currently unknown.

In the light of these findings, we asked here whether ERRα is involved in breast cancer bone metastasis formation and progression, and whether modulating its activity abrogates bone destruction.

Materials and Methods

Ethics statement

BALB/c and NMRI mice were purchased from Charles River laboratories. All procedures involving animals, including housing and care, the method by which they were killed, and experimental protocols, were conducted in accordance with a code of practice established by the local ethical committee (CREEA: comite Regionale d'Ethique pour l'Expérimentation Animale). Studies involving human primary breast tumors were carried out according to the principles embodied in the Declaration of Helsinki. Patients were included anonymously in this study. All human experiments were approved by the Experimental Review Board from the Laennec School of Medicine.

Breast cancer tissue specimens

The autopsy files of the Department of Pathology (Pr. J. Boniver, Centre Hospitalier Universitaire of Liège, Belgium) were searched for diagnosis of disseminated breast cancer with histologically proven bone metastasis during the period 1991 to 1998. Slides were retrieved, and clinical history was obtained. Two breast cancer patients who died with disseminated disease, including bone metastasis, were selected for immunohistochemistry. Soft tissue metastasis (TM) was fixed with formalin, dehydrated, and paraffin embedded.

Breast cancer cohort of patients

In the cohort, patients ($n = 251$) were selected according to the following criteria: primary breast tumor without inflammatory features and no previous treatment (31). Breast cancer tissue biopsies were obtained by surgery, selected by the pathologist, and immediately stored in liquid nitrogen until processing. The biopsies were pulverized using a MikroDismembrator (B.Braun Biotech International), and total RNA was extracted using TRI Reagent (Sigma). RNA quality was verified using an Agilent Bioanalyser 2100 (Agilent Technologies). Real-time reverse transcriptase PCR (RT-PCR) was carried out.

Cell lines and transfection

MDA-BO2-FRT (BO2) cells and stably transfected clonal derivatives were cultured in complete Dulbecco's modified Eagle's medium (Invitrogen), 10% FBS (Perbio), and 1% penicillin/streptomycin (Invitrogen) at 37°C in a 5% CO_2 incubator. Characteristics of MDA-MB-231/BO2-FRT (BO2) breast cancer cells were previously described (32). To avoid potential effects of different insertion sites, a pcDNA5/FRT vector (Invitrogen) was used to obtain the stable BO2-ERRαWT, BO2-ERRαΔAF2, and BO2 (CT) cell lines. Human ERRα cDNA [wild type (WT) and ΔAF2-AD] was obtained from mRNA extracted from BO2-FRT cells, by using RT-PCR with specific primers [(NM_004451.3): *ERRα* upstream (177bp): GGG AAG CTT AGC GCC ATG TCC AGC CAG; *ERRα* downstream (WT; 177-1461 bp): GGG GGA TCC CCA CCC CTT GCC TCA GTC C; *ERRα* downstream (ΔAF2-AD): GGG GGA TCC TCA TGT CTG GCG GAG GAG (177-1350 bp; helix11-12 deletion (32 amino acids)]. Amplimers were sequenced for verification. The pcDNA5/FRT/ERRα-WT and pcDNA5/FRT/ERRα-ΔAF2-AD constructs were cotransfected with the plasmid POG44 (Invitrogen) conferring the specific integration into the FRT site present in the BO2 cells. For clonal selection, cells were cultured for 4 weeks in the presence of hygromycin (20 mg/mL; Invitrogen). Conditioned medium from all clones and from BO2 treated with the inverse agonist XCT-790 at 5.10^{-7} mol/L (Sigma) was obtained after 48 hours in α-MEM supplemented with 0.5% of serum, then filter sterilized and proteins quantified to use equal concentration of proteins for each condition (25 μg).

Animal studies

Tumor fat pad experiments were carried out using BO2-ERRαWT-1, BO2-ERRαΔAF2 (pool of AF2-1, -2, and -3 clones), and BO2 (CT1/2) cell lines (10^6 cells in 50 μL of PBS) injected into the fat pad of the fourth mammary gland of female 4-week-old NMRI nude mice (Charles River). Tumor progression was followed by bioluminescence (NightOwl, Berthold), then tumor size and weight were determined after sacrifice at 66 days.

Bone metastasis experiments using the same pool of clones were carried out in 4-week-old BALB/c nude mice as previously described (33). Cells were suspended at a density of 5×10^5 in 100 μL of PBS and inoculated intravenously into animals. Radiographs (LifeRay HM Plus, Ferrania) of animals were taken at 35 days after inoculation using X-ray (MX-20; Faxitron X-ray Corporation). Animals were sacrificed; hind limbs were collected for histology and histomorphometrics analyses. Tibiae were scanned using microcomputed tomography (Skyscan1076, Skyscan) with an 8.8 voxel size, and three-dimensional (3D) reconstructions were carried out with a dedicated visualization software (Amira 5.2, Visage Imaging Inc.). The area of osteolytic lesions was measured using the computerized image analysis system MorphoExpert (Exploranova). The extent of bone destruction for each animal was expressed in square millimeter.

Bone histomorphometry and histology

Hind limbs from animals were fixed and embedded in paraffin. Five millimeter sections were stained with Goldner's Trichrome and processed for histomorphometric analyses to calculate the bone volume/tissue volume (BV/TV) ratio and the tumor burden/tissue volume (TB/TV) ratio. The *in situ* detection of OC was carried out on sections of bone tissue with metastasis using the tartarte-resistant acid phosphatase (TRAP) activity Kit assay (Sigma). The resorption surface (Oc.S/BS) was calculated as the ratio of TRAP-positive trabecular bone surface (Oc.S) to the total bone surface (BS) using the computerized image analysis system MorphoExpert (Exploranova).

Published OnlineFirst July 6, 2011; DOI:10.1158/0008-5472.CAN-11-1431

Osteoclastogenesis assay

Bone marrow cells from 6-week-old OF1 male mice were cultured for 7 days in differentiation medium: α-MEM medium containing 10% fetal calf serum (Invitrogen), 20 ng/mL of macrophage colony-stimulating factors (M-CSF; R&D Systems), and 200 ng/mL of soluble recombinant receptor activator of nuclear factor κB ligand (RANKL; ref. 34). Cells were continuously (day 1–7) exposed to conditioned medium extracted (25 μg proteins for each conditions) from BO2 clones. After 7 days, mature multinucleated OC were stained for TRAP activity (Sigma-Aldrich) and counted as OC when containing 3 or more nuclei.

Immunofluorescence

BO2 cultures were fixed in culture wells with 3.7% paraformaldehyde (Sigma) in PBS for 10 minutes and permeabilized with 0.2% Triton X-100 in PBS. Immunodetection was carried out using a goat polyclonal antibody against human ERRα (Santa Cruz, Tebu) and the secondary antibody (fluorescein isothiocyanate-conjugated donkey anti-goat; Rockland, Tebu-bio). The distribution of F-actin was visualized using phalloidin (Molecular Probes; ref. 14). Cells were observed using an LMS510 laser scanning confocal microscope (Zeiss) with a 63× (numerical aperture 1.4) Plan Neo Fluor objective.

Immunoblotting

Cell proteins were extracted, separated in 4% to 12% SDS-PAGE (Invitrogen), then transferred to nitrocellulose membranes (Millipore) using a semidry system. For ERRα and α-tubulin detection, the same goat polyclonal antibody ERRα (Santa Cruz) and a mouse polyclonal antibody against human α-tubulin (Sigma-Aldrich) were used. Membrane was incubated with secondary antibody horseradish peroxide (HRP)-conjugated donkey anti-goat (Santa Cruz) and anti-mouse (Amersham), respectively. An ECL kit (PerkinElmer) was used for detection.

Immunocytochemistry

Five micrometer sections were subjected to immunohistochemistry using the same goat polyclonal antibody ERRα (Santa Cruz) and a rabbit polyclonal antibody against human osteoprotegerin (OPG; Abbiotec). Sections were incubated with secondary antibody HRP-conjugated donkey anti-goat and anti-rabbit, respectively (Amersham; dilution 1/300) for 1 hour. After washing, the sections were revealed by 3,3′-diaminobenzidine (Dako).

Real-time RT-PCR

Total RNA was extracted with Trizol reagent (Sigma) from cancer cells and OCs. Real-time RT-PCR was carried out on a

Table 1. Clinical and biological characteristics and *ERRα* mRNA expression in breast cancer patients

Characteristics		All patients $N = 251$			pN0 patients $N = 115$			pN+ patients $N = 136$		
		n	Median	*P*	*n*	Median	*P*	*n*	Median	*P*
Menopausal status	Pre	105	2.68	0.425	48	2.59	0.020	79	3.10	0.229
	Post	146	2.59		67	2.04		57	2.72	
Surgical tumor size	<20 mm	101	2.53		58	2.15		43	2.89	
	≥20 mm	142	2.69	0.256	55	2.46	0.662	87	2.95	0.967
	ND	8								
Histologic type	Ductal	205	2.68		91	2.32		114	3.03	
	Lobular	37	2.09	0.026	16	1.71	0.208	21	2.21	0.058
	Others	9								
Histologic grade[a]	1	27	2.32		14	2.22		13	2.37	
	2	107	2.72		53	2.41		54	3.18	
	3	58	2.84	0.341	22	2.16	0.718	36	3.12	0.040
	ND	13								
Node status	Negative	115	2.31							
	1–3	83	2.72					83	2.72	
	>3	53	3.12	<0.001				53	3.12	0.439
RE status	Negative	42	3.17		16	3.47		26	3.17	
	Positive	209	2.53	<0.001	99	2.12	0.003	110	2.78	0.106
VEGF status[b]	Low	92	2.35		38	1.99		54	2.62	
	High	93	3.08	0.002	42	2.57	0,018	51	3.23	0.010
	ND	66								

NOTE: *P* values correspond to Mann–Whitney test or Kruskall–Wallis test (histologic grade and node status).
[a]Histologic grade defined only in ductal carcinomas.
[b]Low: <50% quartile, high: ≥50% quartile.

Published OnlineFirst July 6, 2011; DOI:10.1158/0008-5472.CAN-11-1431

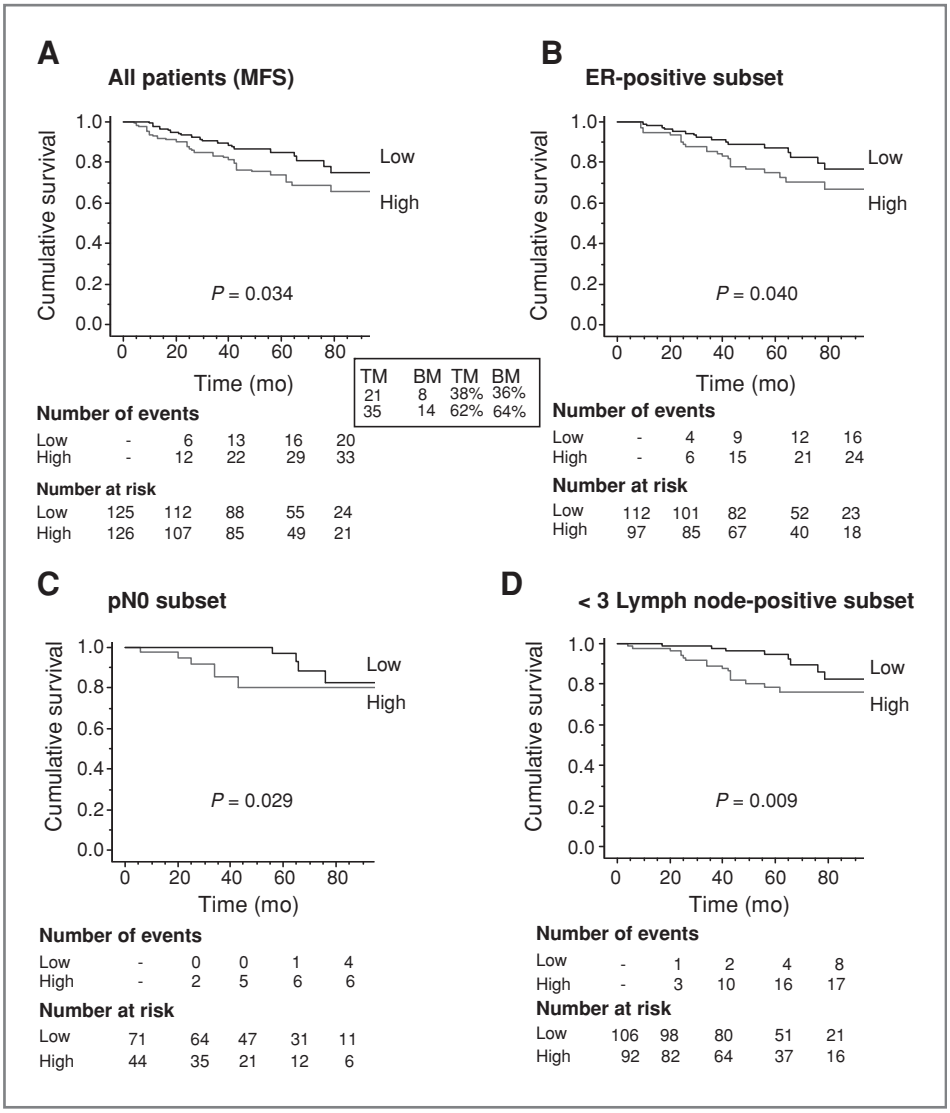

Figure 1. *ERRα* is a bad prognostic marker. Kaplan–Meier curves show correlation between high expression of *ERRα*, categorized with median value, and MFS in patients in (A) the whole population ($N = 251$), (B) the ER-positive subset ($N = 209$), (C and D) the pN0 subset patients ($N = 115$) and the <3 lymph node-positive subset ($N = 198$). Low: ≤50% quartile; high: ≥50%.

Roche Lightcycler Module (Roche) with specific primers (see Supplementary Table S2). Real-time RT-PCR was carried out by using SYBR Green (Qiagen) on the LightCycler system (Roche) according to the manufacturer's instructions. Amplimers were all normalized to corresponding L32 values. Data analysis was carried out using the comparative C_t method.

Real-time RT-PCR on breast cancer tissue biopsy mRNA was carried out using primers specific for human *L32* (101 bp): 5′-CAAGGAGCTGGAAGTGCTGC-3′, 5′-CAGCTCTTTCCACGATGGCT-3′; TATA-box binding protein (*TBP*; 138 bp) 5′-TGGTGTGCACAGGAGCAAG-3′, 5′-TTCACATCACAGCTCCCCAC-3′; *ERRα* (101 bp): 5′-ACCGAGAGATTGTGGTCACCA-3′, 5′-CATCCACACGCTCTGCAGTACT-3′ and *OPG* (Supplementary Table S2) and SYBR green (Invitrogen) in 96-well plates on a Mastercycler EP system (Realplex2, Eppendorf) according to the manufacturer's instructions with an initial step for 10 minutes at 95°C followed by 40 cycles of 20 seconds at 95°C, 15 seconds at T_m (*L32*: 62°C, *TBP*: 67°C, *ERRα*: 59°C), and 10 seconds at 72°C. *ERRα* and *OPG* expression were normalized with the average of the genes expression encoding the ribosomal protein *L32* and the *TBP*.

Cell invasion assay

Invasion assays were carried out using Bio-Coat migration chambers (Becton Dickinson) with 8 μm filters coated with Matrigel as described previously (35). BO2 cells (5×10^4) were plated in the upper chambers and the chemoattractant (10% FBS) in the lower chambers. After 24 hours at 37°C in 5% CO_2 incubator, cells that had migrated through the filters were fixed and stained. Cells were counted (200× magnification). All experiments were run in triplicate, and invasion was expressed in cells/square millimeter.

OPG ELISA

Conditioned medium obtained from BO2-CT(1/2), BO2-ERRα-WT-1, and BO2-FRT-ERRαΔAF2 (pool of AF2-1, -2

Published OnlineFirst July 6, 2011; DOI:10.1158/0008-5472.CAN-11-1431

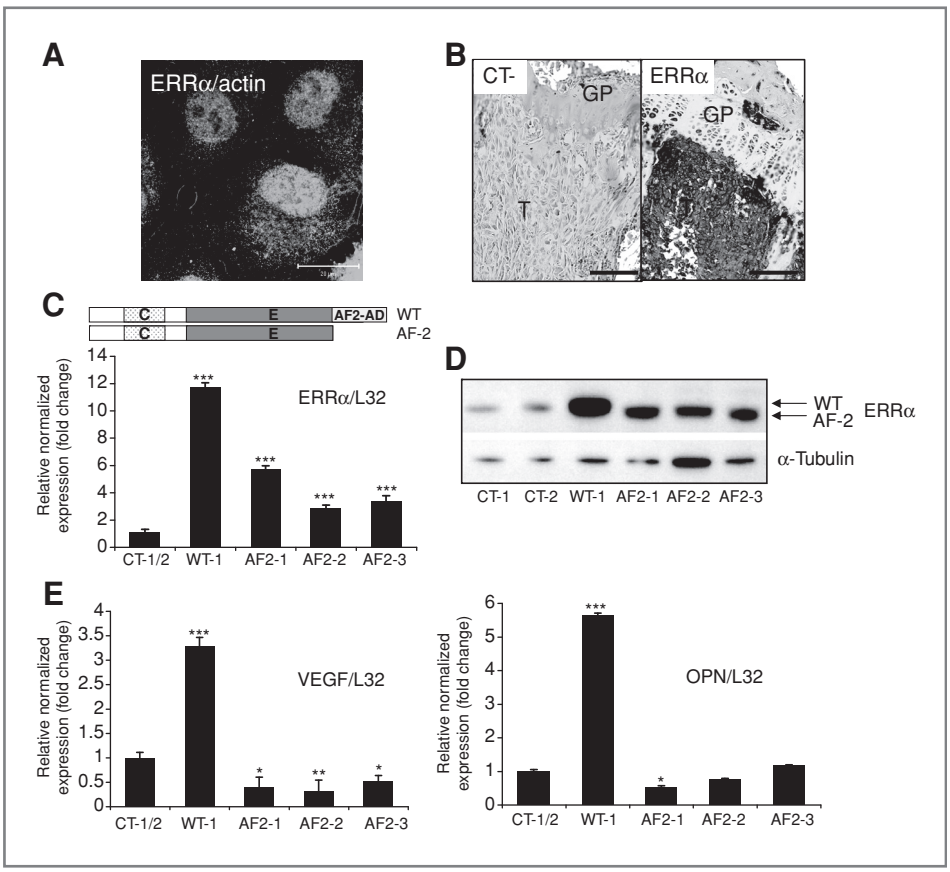

Figure 2. Modulation of ERRα in BO2 breast cancer cell line. A, ERRα protein expression (nucleus and cytoplasm) in BO2 cells by immunofluorescence and confocal microscopy and (B) *in vivo* by immunohistochemistry in bone metastasis present 30 days after intravenous injection of BO2 cells. C, isolation after stable transfection of three independent BO2-ERRαΔAF2 clones (ERRα dominant-negative form), one clone BO2-ERRαWT and two controls (CT-1 and CT-2) BO2-CT (empty vector). *ERRα* expression was assessed by real-time PCR on triplicate samples and normalized against that of the ribosomal protein gene *L32* (ANOVA, $P < 0.0001$) and (D) by Western blotting. (E) *VEGF* and *OPN* expression was increased in BO2-ERRαWT and decreased or not regulated in BO2-ERRαΔAF2 (ANOVA, $P < 0.0001$ for VEGF and OPN in WT-1 or ΔAF2 versus CT). (A) bar = 20 μm and (B) bar = 200 μm. T, tumor; GP, growth plate.

and -3 clones) were diluted following the manufacturer's instructions, and OPG concentration was evaluated using the ELISA Kit (RayBiotech).

Statistical analysis

Data were analyzed statistically by one-way ANOVA followed by post hoc *t*-tests to assess the differences between groups for *in vitro* and *in vivo* studies. Concerning the cohort, the median follow-up at the time of analysis was 54 months. The criterion for statistical analyses was the metastasis free survival (MFS), that is, the delay between the time of primary surgery and the first event: nodal or distant metastasis or death. Analysis of the distribution of ERRα expression in relation to the usual prognostic parameters was carried out using the Mann–Whitney or Kruskall–Wallis test. Survival probabilities were estimated using Kaplan–Meier estimators and were compared using the log-rank test. Univariate analysis was carried out using the Cox proportional hazard model. Results of $P < 0.05$ were considered significant.

Results and Discussion

ERRα mRNA and protein expression in human primary breast tumors and bone metastasis

We analyzed *ERRα* mRNA expression by real-time RT-PCR in a cohort of 251 breast tumor biopsies (Supplementary Table S1; ref. 31). As reported previously by others (14, 15, 17, 18), a statistically significant association was detected in all patients analyzed between *ERRα* expression and histologic type, node status, and ERs (radioligand method; $P = 0.026$, $P < 0.001$, $P < 0.001$; Table 1). The Kaplan–Meier curve was constructed after segmentation into 2 groups on the basis of the median value for *ERRα* expression (Fig. 1A–D). It was observed that high levels of *ERRα* mRNA expression were related to a decrease in MFS ($N = 251$, $P = 0.034$; Fig. 1A). Sixty-two percent of patients (35/56) with high *ERRα* expression levels exhibited liver, lung, bone, and soft tissue metastasis compared with 38% of patients (21/56) having low *ERRα* levels (Fig. 1A, see frame). This paralleled the frequencies seen in patients ($n = 22$) who had developed "only" bone metastasis (BM), that is, 64% (high *ERRα*) and 36% (low *ERRα*; Fig. 1A) suggesting that *ERRα* is an overall bad prognostic factor that is not a determinant of metastasis location of breast cancer cells. Moreover, high *ERRα* expression correlated with a higher risk of recurrence at an early stage of the disease in the ER-positive group ($N = 209$), the pN0 subset, and in the pN < 3 lymph-node-positive subset ($P = 0.04$; $P = 0.029$, and $P = 0.009$; log-rank test), when compared with low *ERRα* (Fig. 1B–D) suggesting that *ERRα* may be a very useful early prognostic marker in breast cancer. Finally, as previously described (15), ERRα protein was present *in situ* and in invasive breast carcinoma cells (Supplementary Fig. S1B and C, respectively)

Published OnlineFirst July 6, 2011; DOI:10.1158/0008-5472.CAN-11-1431

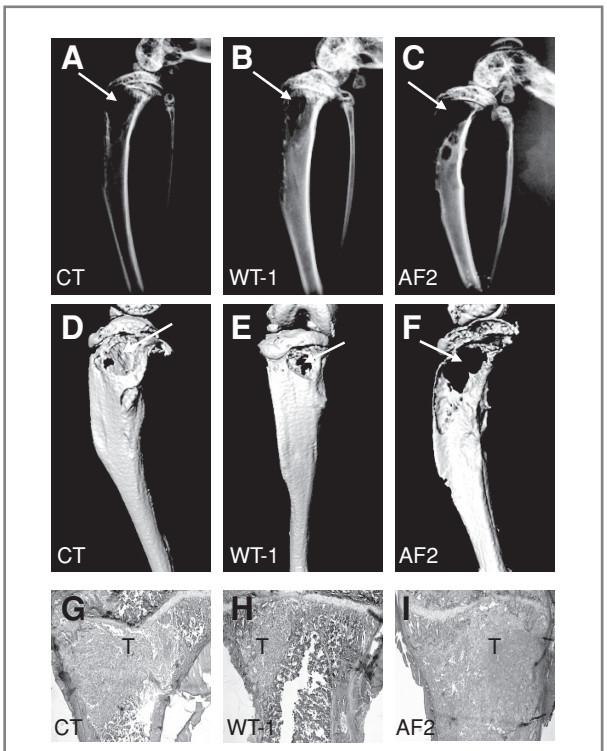

J

BO2-FRT Clones	CT	ERRα WT	ERRα ΔAF
Radiography (mm^2/animal)	10.9 ± 1.9 (n = 9)	7.1 ± 3.4* (n = 8)	30.7 ± 7.2*** (n = 9)
Bone volume (BV/TV, %)	11.4 ± 1.1 (n' = 13)	15.1 ± 0.9* (n' = 13)	6.4 ± 0.4*** (n' = 14)
Tumor burden (TB/STV, %)	35.9 ± 4.2 (n' = 13)	21 ± 4.8* (n' = 13)	71 ± 3.2*** (n' = 14)
Osteolyse (Oc.S/BS, %)	49.3 ± 3.4 (n' = 14)	21 ± 5.6** (n' = 13)	70 ± 6*** (n' = 16)

Figure 3. Overexpression of ERRα inhibits development of bone metastasis. A–C, BO2-ERRαWT-1, BO2-ERRαΔAF2 (pool), or BO2-CT (pool) cells were inoculated into BALB/c nude mice; 35 days postinoculation, radiography revealed smaller osteolytic lesions in mice injected with BO2-ERRαWT-1 cells and much larger lesions in mice injected with BO2-ERRαΔAF2 cells compared with mice injected with CT cells (see white arrows). D–F, 3D micro-CT reconstructions of tibiae and (G–J) histology after Goldner's Trichrome staining confirmed the radiography results. J, quantification of bone destruction. T, tumor.

but not in normal breast epithelial cells (Supplementary Fig. S1A). ERRα was also clearly present in breast cancer cells that metastasized to bone (Supplementary Fig. S1D see T). As previously reported by us (21), ERRα was also detected in osteocytes embedded in the bone matrix.

ERRα expression in breast cancer cells reduces their ability to induce osteolytic lesions *in vivo*

To assess whether ERRα is involved in bone metastasis formation, we used MDA-BO2-FRT (BO2) cells, a subpopulation of the human MDA-231 breast cancer cell line, that was selected for the high efficiency with which it metastasizes to bone (32). ERRα protein was seen in the nucleus and cytoplasm of BO2 cells *in vitro* (Fig. 2A) and *in situ* in bone metastasis from legs of animals, 30 days after intravenous tumor cell inoculation (Fig. 2B).

To establish a functional role for ERRα in bone metastasis development, we next transfected B02 cells with a full-length (WT) ERRα or a truncated version of ERRα lacking the coactivator binding domain AF2, ERRαΔAF2, which acts as a dominant-negative form (22, 23, 36; Fig. 2C). Constructs of human ERRαWT and ERRαΔAF2 were stably transfected into the genomic FRT site present in the BO2 cells. Three independent BO2-ERRαΔAF2 (1, 2, 3), one BO2-ERRαWT, and two BO2-CT (empty vector) clones were obtained, named AF2-1, AF2-2, AF2-3, WT-1, CT-1, and CT-2, respectively. As judged by real-time PCR, total ERRα mRNA expression was increased when compared with CT-1/2 clones (Fig. 2C). Western blotting detected a band of approximately 50 kD for ERRα protein in CT1-2 and WT-1 that was increased in WT-1 and AF2-1, AF2-2, and AF2-3 cells. The presence of a band with a slightly lower molecular weight in AF2-1, AF2-2, and AF2-3 cells corresponded well with the expected size for truncation of the AF2 domain (42 amino acids; Fig. 2D). mRNA expression levels of the ERRα target genes *VEGF* and *OPN* were statistically significantly increased in WT-1 cells compared with CT-1/2 cells (Fig. 2E). By contrast, *VEGF* and *OPN* mRNA levels remained reduced or unchanged in AF2 clones (Fig. 2E), confirming the increased activity and the dominant-negative functions of the WT and truncated ERRαΔAF2 constructs, respectively.

To assess the involvement of ERRα in bone metastasis formation, CT (pool of CT-1 and -2 clones), WT-1, and AF2 (pool of AF2-1, -2 and -3 clones) cells were inoculated intravenously into female BALB/c nude mice. Thirty-five days after tumor cell injection, radiographic analysis revealed that animals bearing WT-1 tumors had osteolytic lesions that were 40% smaller than those of mice bearing CT tumors (Fig. 3A,B, and J). By contrast, there was a 3-fold increase in the extent of osteolytic lesions in animals bearing AF2 tumors, when compared with control (Fig. 3A, C, and J). The inhibitory effect of ERRα on cancer-induced bone destruction was confirmed using 3D micro-CT reconstruction (Fig. 3D–F), histology (Fig. 3G–I), and histomorphometric analyses of tibiae (BV/TV; skeletal tumor burden, TB/STV; Fig. 3J). Taken together, our results indicated that overexpression of ERRα in breast cancer cells reduced the formation of osteolytic lesions.

Regulation of OC formation by ERRα–expressing BO2 cells

Given these data, we next asked whether modulation of ERRα in breast cancer cells could alter OCs, the bone resorbing cells. TRAP staining of tibial sections of metastatic legs from animals bearing WT-1 and AF2 tumors showed a 43% decrease and a 143% increase of TRAP-positive OC surface (Oc.S/BS) at the bone/tumor cell interface, respectively, when compared with CT tumors (Fig. 4A and 3J; Supplementary Fig. S2). Consistent with these *in vivo* data, the treatment of primary mouse bone marrow cell

Published OnlineFirst July 6, 2011; DOI:10.1158/0008-5472.CAN-11-1431

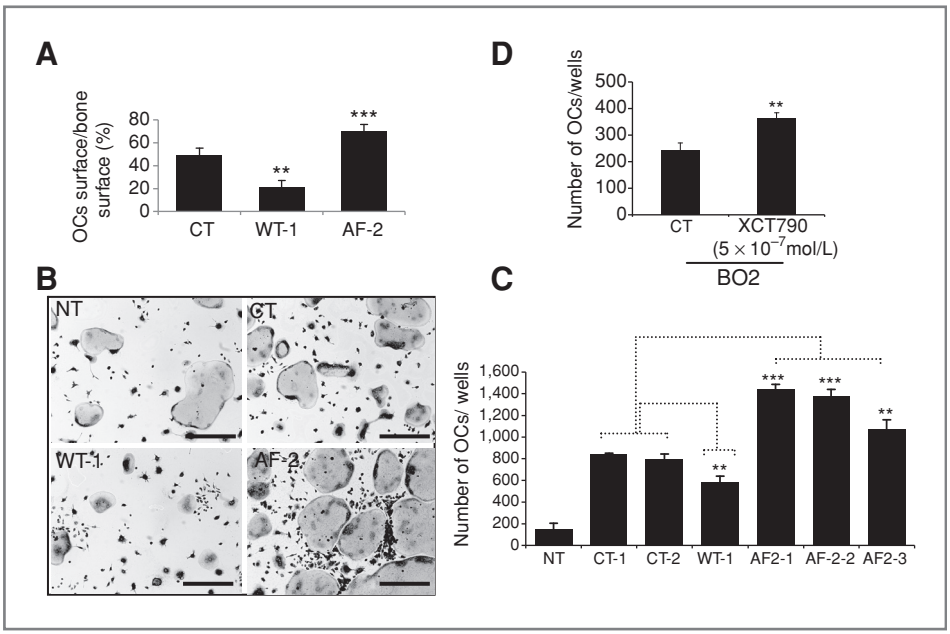

Figure 4. ERRα expression in BO2 cells regulates OCs formation. A, TRAP staining of OCs in sections of tibiae taken from mice injected with BO2-ERRαWT-1, BO2-ERRαΔAF2 (pool), or BO2-CT (pool) cells shows decreased and increased surface of OCs in BO2-ERRαWT-1 and BO2-ERRαΔAF2, respectively compared with CT (ANOVA, $P < 0.0001$). B and C, primary mouse bone marrow cells were cultured in the presence of RANKL and M-CSF and treated or not with medium conditioned by BO2-ERRαWT-1, BO2-ERRαΔAF2, or BO2-CT cells. Fewer OCs formed in cultures treated with BO2-ERRαWT-1 conditioned medium, whereas more formed in cultures treated with BO2-ERRαΔAF2 conditioned medium, compared with CT (refs. 1, 2) conditioned medium (ANOVA, $P < 0.0001$). D, conditioned medium obtained from parental BO2 cells treated with the ERRα inverse agonist XCT-790 increased OCs formation, mimicking the results obtained with BO2-ERRαΔAF2 conditioned medium (ANOVA, $P < 0.001$). Bar, 100 μm.

cultures with RANKL and M-CSF together with the conditioned medium of WT-1 cells inhibited the formation of TRAP-positive multinucleated OCs compared with that observed with the conditioned medium of CT cells (Fig. 4B and C). By contrast, the conditioned medium from AF2 cells stimulated OC formation (Fig. 4B and C). In addition, the conditioned medium from parental BO2 cells treated with the inverse agonist XCT-790, which blocks ERRα activity, increased OC formation compared with control (dimethyl sulfoxide; Fig. 4D), confirming our osteoclastogenesis data obtained with the conditioned medium of AF2 cells.

ERRα regulates OPG expression in breast cancer cells

We showed that B02 breast cancer cells overexpressing wild-type ERRα markedly inhibited osteolysis *in vivo* (Fig. 3J) and reduced OC formation *in vitro* (Fig. 4). We quantified several markers involved in osteoblasts and OC differentiation, and we found that the *OPG*, a soluble decoy receptor for RANKL that inhibits osteoclastogenesis, was regulated by ERRα (Fig. 5A; ref. 37). By immunohistochemistry, we show that OPG expression was higher in skeletal WT-1 tumors compared with that observed in AF2 and CT tumors (Fig. 5B). In addition, as judged by ELISA, WT-1 cells secreted higher amounts of OPG compared with CT-1/2 and AF2 cells (pool of AF2-1, -2 and -3 clones; Fig. 5C). *OPG* mRNA expression was also quantified by real-time RT-PCR in the cohort of 251 patients. *OPG* levels were statistically significantly higher in *ERRα*-positive tumors compared with *ERRα*-negative tumors (Fig. 5D; $P = 0.013$). Moreover, there was a positive correlation between high mRNA expression levels of both *ERRα* and *OPG* (*ERRα*$^+$/*OPG*$^+$) and a decrease in relapse-free survival ($P = 0.028$, log-rank test; Fig. 5E). All together, the significant correlation between high *ERRα* and *OPG* in patients and the regulation of *OPG* by ERRα in BO2 cells provide a mechanistic basis for the reduction of osteoclastogenesis *in vitro* and *in vivo*. Interestingly, *OPG* in our preclinical data suggest that, alone it had no prognostic value in breast carcinomas (Fig. 5F) whereas in association with high *ERRα* mRNA levels, a correlation with a poor clinical outcome in patients was found (Fig. 5E). OPG is not only an osteoclastogenesis inhibitor, but also a survival factor for human breast cancer cells (38, 39). It also promotes angiogenesis (40), and its overexpression in human MCF-7 breast cancer cells enhances tumor growth following orthotopic inoculation in animals (41). ERRα has been implicated in tumor progression, and the positive association between high *ERRα*/*OPG* mRNA levels and increased risk of recurrences in patients (Fig. 5E) suggested that ERRα could play a role on primary tumor expansion.

ERRα stimulates tumor growth and angiogenesis *in vivo*

To address this hypothesis, orthotopic tumors were induced with CT (pool of CT-1 and -2 clones), WT-1, or AF2 (pool of AF2-1, -2 and -3 clones) cells upon inoculation within the mammary fat pad of NMRI nude female mice.

Published OnlineFirst July 6, 2011; DOI:10.1158/0008-5472.CAN-11-1431

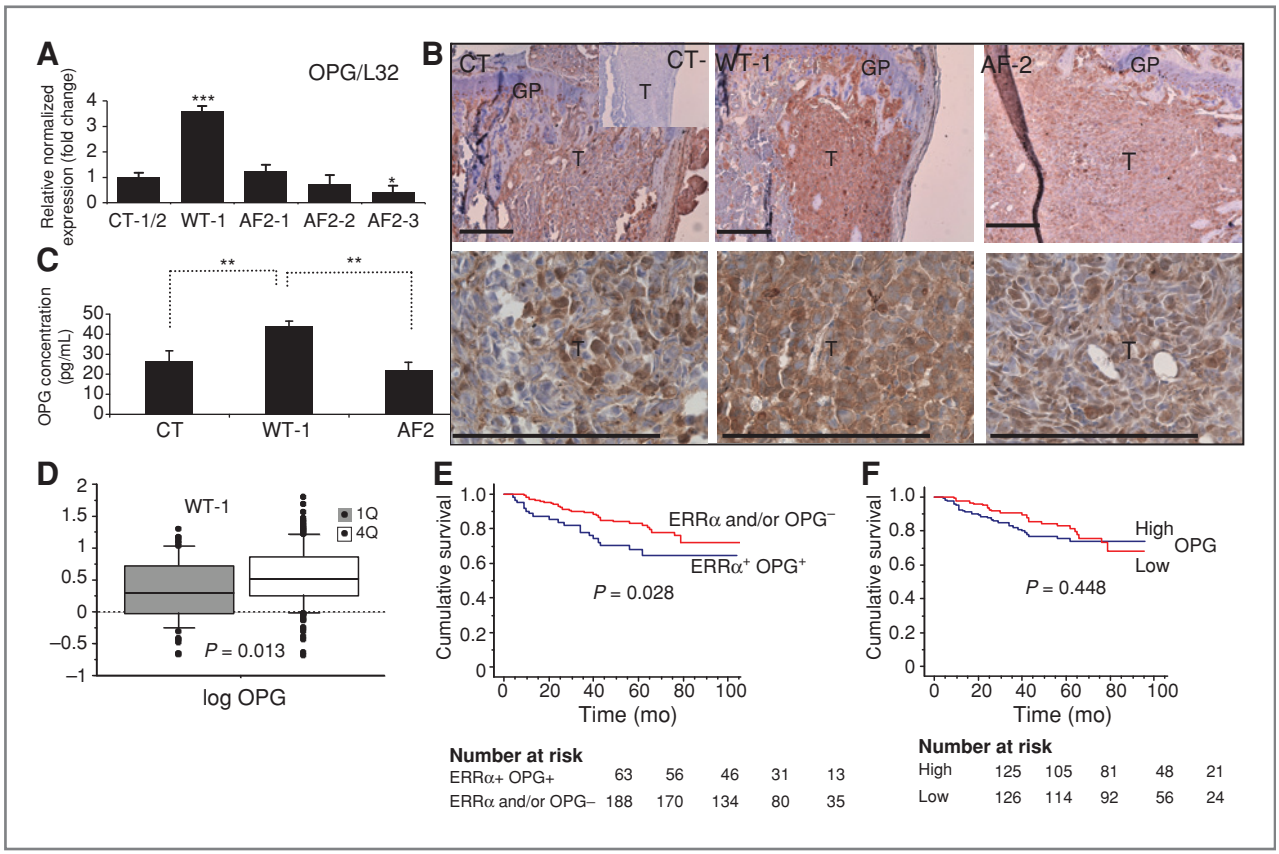

Figure 5. Correlation of ERRα and OPG in BO2 cells and breast cancer patients. A, real-time PCR carried out on RNA extracted from BO2 clones showed increased expression of *OPG* by ERRα (ANOVA, $P < 0.0001$). B, staining for OPG is higher in bone metastasis induced by BO2-ERRαWT cells compared with BO2-CT and BO2-ERRαΔAF2 cells; tissues collected 35 days postcell inoculation. C, ELISA quantification confirmed the increased secretion of OPG by BO2-ERRαWT compared with BO2-CT (pool) and BO2-ERRαΔAF2 (pool) cells (ANOVA, $P = 0.0064$; $P < 0,01$ CT versus WT-1 and WT-1 versus AF-2). D and E, a significant correlation was also found between levels of ERRα mRNA and median values of OPG mRNA in the cohort (ERRα 1st quartile and median OPG = 2.03; ERRα 2nd–4th quartile and median OPG = 3.45). Kaplan–Meier curves show that ERRα$^+$/OPG$^+$ expression was associated with a decrease in MFS. F, OPG alone was not associated with MFS.

Bioluminescence analysis from day 5 to day 66 revealed a dramatically greater tumor progression in WT-1 tumor-bearing animals compared with that observed with CT and AF2 tumor-bearing animals a modest increase in AF2 tumor burden was also observed at day 62 and 66 (Fig. 6A and B). Tumor weight/size at day 66 (Fig. 6C and D) correlated well with bioluminescence quantification (Fig. 6B and C). Interestingly, WT-1 tumors were highly vascularized compared with CT and AF2 tumors (Fig. 6E), an observation correlating with higher *VEGF* mRNA levels observed in WT-1 versus AF2 or CT tumors (Fig. 6E). Moreover, if these results are in agreement with previous data describing *VEGF* as a target gene for ERRα in breast cancer (42), we show for the first time a positive association between high levels of *ERRα* and *VEGF* in breast tumors from patients ($P = 0.002$; Table 1). Interestingly, OPG expression that can be stimulated by VEGF in endothelial cells, is also known to be a positive regulator of microvessel formation *in vivo* (43) and therefore can participate to the neovascularization observed in WT-1 tumors. We also observed that ERRα promoted BO2 breast cancer cell invasion *in vitro* (Supplementary Fig. S3A) but has a slightly effect on proliferation (data not shown). Consistent with this we found matrix metalloproteinases *MMP1* and *MMP13* regulated by ERRα (Supplementary Fig. S3B). These results were in agreement with previous findings showing that the silencing of ERRα dramatically reduced the *in vitro* migratory capacity of breast cancer cell lines (44). Taken together, these results strongly suggested that ERRα promoted tumor growth, mainly through the stimulation of angiogenesis and invasion. Based on our results on high ERRα/OPG/VEGF in our preclinical study, we propose that OPG worked in concert with VEGF to stimulate tumor angiogenesis which, in turn, promoted the growth of BO2-ERRαWT cells. Conversely, in bone metastasis although the angiogenic factor *VEGF* was overproduced in BO2-ERRαWT cells, tumor-derived VEGF had probably a low impact on progression of osteolytic lesions. Indeed, recent studies have shown that hypoxia was nonessential for bone metastasis while promoting angiogenesis in lung metastasis and primary tumor

Published OnlineFirst July 6, 2011; DOI:10.1158/0008-5472.CAN-11-1431

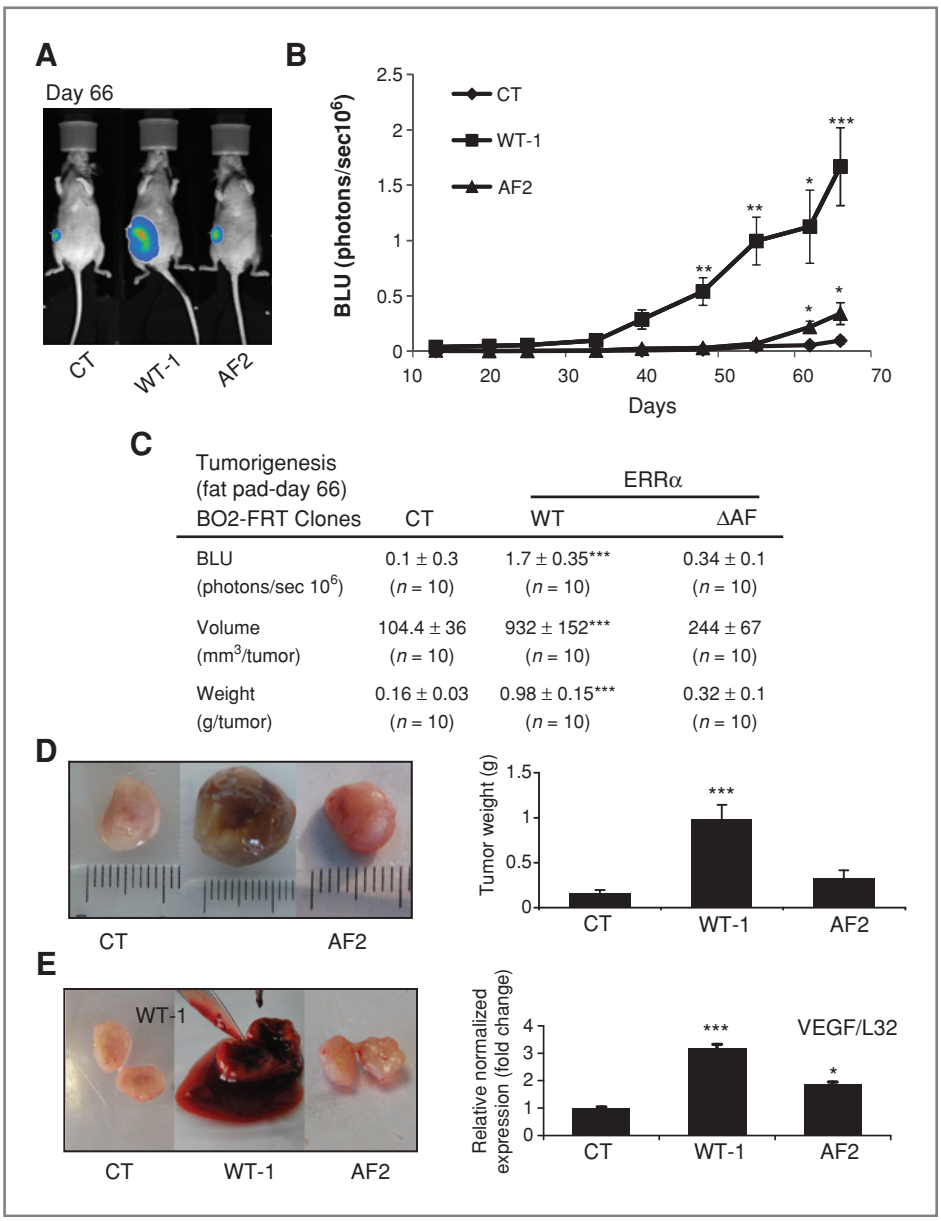

Figure 6. Stimulation of tumor progression and angiogenesis by ERRα *in vivo*. A–C, BO2-ERRαWT, BO2-ERRαΔAF2 (pool), or BO2-CT (pool) cells were inoculated into the fat pad of NMRI nude mice. Tumor progression was followed by bioluminescence from day 5 to 66. Greater tumor expansion was observed in mice with BO2-ERRαWT-1 compared with BO2-ERRαΔAF2 (pool) or BO2-CT (pool) cells. C and D, weight and volume of tumors dissected at endpoint (E) and *VEGF* expression normalized against *L32* (ANOVA, $P < 0.001$) within tumors (pool of $n = 3$ for each condition) correlated with greater tumor vascularization.

growth (45). Therefore, modulating angiogenesis through VEGF and the proangiogenic role of OPG may have no impact on angiogenesis in bone, as bone is already extremely vascularized (46), but have dramatic impact on vascularization and progression of primary breast tumors or metastasis to nonbone sites. These data provide novel insights into how ERRα can be a bad prognostic factor in the primary tumor (angiogenesis via VEGF and OPG) but a favorable biomarker in the very special case of bone metastasis (inhibition of OC formation through OPG).

In conclusion, our results show for the first time that ERRα plays a dual role, promoting the progression and invasion of primary tumors, but decreasing osteolytic lesions in bone. In addition, our data show that OPG is modulated by ERRα that probably contributes to the overall negative clinical outcome which is associated with the expression of ERRα in human breast carcinomas.

Disclosure of Potential Conflicts of Interest

No potential conflicts of interest were disclosed.

Acknowledgments

We are very grateful to C. Lionnet and C. Chamot from PLATIM (IFR 128 Lyon Biosciences) for their help with imaging experiments and to Blandine Deux, Vincent Gonin, and Pascale Heneaux for their technical help. The authors also thank the CeCIL platform (Faculté de Médecine Laennec, Lyon, France) for technical assistance.

Published OnlineFirst July 6, 2011; DOI:10.1158/0008-5472.CAN-11-1431

Grant Support

This work was supported by the CNRS (EB), Inserm, the University of Lyon, "Ligue Regionale contre le Cancer" (Isère; E. Bonnelye). A. Fradet is supported by the Ligue Nationale contre le Cancer, B. Depalle by region Rhône Alpes, and A. Bellahcène from the National Fund for Scientific Research, Belgium.

The costs of publication of this article were defrayed in part by the payment of page charges. This article must therefore be hereby marked *advertisement* in accordance with 18 U.S.C. Section 1734 solely to indicate this fact.

Received April 29, 2011; revised June 29, 2011; accepted June 29, 2011; published OnlineFirst July 6, 2011.

References

1. Roodman GD. Mechanisms of bone metastasis. N Engl J Med 2004;350:1655–64.
2. Kozlow W, Guise TA. Breast cancer metastasis to bone: mechanisms of osteolysis and implications for therapy. J Mammary Gland Biol Neoplasia 2005;10:169–80.
3. Clezardin P, Teti A. Bone metastasis: pathogenesis and therapeutic implications. Clin Exp Metastasis 2007;24:599–608.
4. Clezardin P. Bisphosphonates' antitumor activity: An unravelled side of a multifaceted drug class. Bone Epub2010 Jul 22.
5. Benoit G, Cooney A, Giguere V, Ingraham H, Lazar M, Muscat G, et al. International Union of Pharmacology. LXVI. Orphan nuclear receptors. Pharmacol Rev 2006;58:798–836.
6. Kallen J, Schlaeppi JM, Bitsch F, Filipuzzi I, Schilb A, Riou V, et al. Evidence for ligand-independent transcriptional activation of the human estrogen-related receptor alpha (ERRalpha): crystal structure of ERRalpha ligand binding domain in complex with peroxisome proliferator-activated receptor coactivator-1alpha. J Biol Chem 2004;279:49330–7.
7. Greschik H, Wurtz JM, Sanglier S, Bourguet W, van Dorsselaer A, Moras D, et al. Structural and functional evidence for ligand-independent transcriptional activation by the estrogen-related receptor 3. Mol Cell 2002;9:303–13.
8. Giguere V, Yang N, Segui P, Evans RM. Identification of a new class of steroid hormone receptors. Nature 1988;331:91–4.
9. Busch BB SWJ, Martin R, Ordentlich P, Zhou S, Sapp DW, Horlick RA, et al. Identification of a selective inverse agonist for the orphan nuclear receptor estrogen-related receptor alpha. J Med Chem 2004;47: 5593–6.
10. Willy PJ, Murray IR, Qian J, Busch BB, Stevens WC, Martin R, et al. Regulation of PPARgamma coactivator 1alpha (PGC-1alpha) signaling by an estrogen-related receptor alpha (ERRalpha) ligand. Proc Natl Acad Sci U S A 2004;101:8912–7.
11. Lui K TT, Mori T, Zhou D, Chen S. MCF-7aro/ERE, a novel cell line for rapid screening of aromatase inhibitors, ERalpha ligands and ERRalpha ligands. Biochem Pharmacol 2008;76:208–15.
12. Luo J, Sladek R, Carrier J, Bader JA, Richard D, Giguere V. Reduced fat mass in mice lacking orphan nuclear receptor estrogen-related receptor alpha. Mol Cell Biol 2003;23:7947–56.
13. Huss JM, Imahashi K, Dufour CR, Weinheimer CJ, Courtois M, Kovacs A, et al. The nuclear receptor ERRalpha is required for the bioenergetic and functional adaptation to cardiac pressure overload. Cell Metab 2007;6:5–37.
14. Ariazi EA, Clark GM, Mertz JE. Estrogen-related receptor alpha and estrogen-related receptor gamma associate with unfavorable and favorable biomarkers, respectively, in human breast cancer. Cancer Res 2002;62:6510–8.
15. Suzuki T, Miki Y, Moriya T, Shimada N, Ishida T, Hirakawa H, et al. Estrogen-related receptor alpha in human breast carcinoma as a potent prognostic factor. Cancer Res 2004;64:4670–6.
16. Cheung CP, Yu S, Wong KB, Chan LW, Lai FM, Wang X, et al. Expression and functional study of estrogen receptor-related receptors in human prostatic cells and tissues. J Clin Endocrinol Metab 2005;90:1830–44.
17. Gao M, Sun P, Wang J, Zhao D, Wei L. Expression of estrogen receptor-related receptor isoforms and clinical significance in endometrial adenocarcinoma. Int J Gynecol Cancer 2006;16: 827–33.
18. Cavallini A, Notarnicola M, Giannini R, Montemurro S, Lorusso D, Visconti A, et al. Oestrogen receptor-related receptor alpha (ERRalpha) and oestrogen receptors (ERalpha and ERbeta) exhibit different gene expression in human colorectal tumour progression. Eur J Cancer 2005;41:1487–94.
19. Sun P, Sehouli J, Denkert C, Mustea A, Könsgen D, Koch I, et al. Expression of estrogen receptor-related receptors, a subfamily of orphan nuclear receptors, as new tumor biomarkers in ovarian cancer cells. J Mol Med 2005;83:457–67.
20. Stein RA, McDonnell DP. Estrogen-related receptor {alpha} as a therapeutic target in cancer. Endocr Relat Cancer 2006;13 Suppl 1: S25–32.
21. Bonnelye E, Merdad L, Kung V, Aubin JE. The orphan nuclear estrogen receptor–related receptor (ERR) is expressed throughout osteoblast differentiation and regulates bone formation in vitro. J Cell Biol 2001;153:971–83.
22. Bonnelye E, Zirngibl RA, Jurdic P, Aubin JE. The orphan nuclear estrogen receptor-related receptor-{alpha} regulates cartilage formation *in vitro*: implication of Sox9. Endocrinology 2007;148:1195–205.
23. Bonnelye E, Saltel F, Chabadel A, Zirngibl RA, Aubin JE, Jurdic P. Involvement of the orphan nuclear estrogen receptor-related receptor ERRalpha in osteoclast adhesion and transmigration. J Mol Endocrinol 2010;45:365–77.
24. Rajalin AM PH, Aarnisalo P. ERRalpha regulates osteoblastic and adipogenic differentiation of mouse bone marrow mesenchymal stem cells. Biochem Biophys Res Commun 2010;396:477–82.
25. Delhon I, Gutzwiller S, Morvan F, Rangwala S, Wyder L, Evans G, et al. Absence of estrogen receptor related alpha increases osteoblastic differentiation and cancellous bone mineral density. Endocrinology 2009;150:4463–72.
26. Teyssier CGM, Rabier B, Monfoulet L, Dine J, Macari C, Espallergues J, et al. Absence of ERRalpha in female mice confers resistance to bone loss induced by age or estrogen-deficiency. PLoS One 2009;4: e7942.
27. Wei W WX, Yang M, Smith LC, Dechow PC, Sonoda J, Evans RM, et al. PGC1beta mediates PPARgamma activation of osteoclastogenesis androsiglitazone-induced bone loss. Cell Metab 2010;11:503–16.
28. Bonnelye E, Vanacker JM, Dittmar T, Begue A, Desbiens X, Denhardt DT, et al. The ERR-1 orphan receptor is a transcriptional activator expressed during bone development. Mol Endocrinol 1997;11:905–16.
29. Vanacker JM, Delmarre C, Guo X, Laudet V. Activation of the osteopontin promoter by the orphan nuclear receptor estrogen receptor related alpha. Cell Growth Differ 1998;9:1007–14.
30. Zirngibl RA CJ, Aubin JE. Estrogen receptor-related receptor alpha (ERRalpha) regulates osteopontin expression through a non-canonical ERRalpha response element in a cell context-dependent manner. J Mol Endocrinol 2008;40:61–73.
31. Berthier ASS, Sasco AJ, Bobin JY, De Laroche G, Datchary J, Saez S, et al. High expression of gabarapl1 is associated with a better outcome for patients with lymph node-positive breast cancer. Br J Cancer 2010;102:1024–31.
32. Peyruchaud O, Winding B, Pecheur I, Serre CM, Delmas P, Clezardin P. Early detection of bone metastases in a murine model using fluorescent human breast cancer cells: application to the use of the bisphosphonate zoledronic acid in the treatment of osteolytic lesions. J Bone Miner Res 2001;16:2027–34.
33. Le Gall CBA, Bonnelye E, Gasser JA, Castronovo V, Green J, Zimmermann J, et al. A cathepsin K inhibitor reduces breast cancer induced osteolysis and skeletal tumor burden. Cancer Res 2007; 67:9894–902.
34. David MWE, Descotes F, Jansen S, Deux B, Ribeiro J, Serre CM, et al. Cancer cell expression of autotaxin controls bone metastasis

Published OnlineFirst July 6, 2011; DOI:10.1158/0008-5472.CAN-11-1431

formation in mouse through lysophosphatidic acid-dependent activation of osteoclasts. PLoS One 2010;5:e9741.
35. Boissier SFM, Peyruchaud O, Magnetto S, Ebetino FH, Colombel M, Delmas P, et al. Bisphosphonates inhibit breast and prostate carcinoma cell invasion, an early event in the formation of bone metastases. Cancer Res 2000;60:2949–54.
36. Vanacker JM, Pettersson K, Gustafsson JA, Laudet V. Transcriptional targets shared by estrogen receptor- related receptors (ERRs) and estrogen receptor (ER) alpha, but not by ERbeta. Embo J 1999;18:4270–9.
37. Boyle WJ, Simonet WS, Lacey DL. Osteoclast differentiation and activation. Nature 2003;423:337–42.
38. Rachner TDBP, Rauner M, Goettsch C, Singh SK, Schoppet M, Hofbauer LC. Osteoprotegerin production by breast cancer cells is suppressed by dexamethasone and confers resistance against TRAIL-induced apoptosis. J Cell Biochem 2009;108:106–16.
39. Malyankar UMSM, Suchland KL, Yun TJ, Clark EA, Giachelli CM. Osteoprotegerin is an alpha vbeta 3-induced, NF-kappa B-dependent survival factor for endothelial cells. J Biol Chem 2000;275:20959–62.
40. McGonigle JSGC, Scatena M. Osteoprotegerin and RANKL differentially regulate angiogenesis and endothelial cell function. Angiogenesis 2009;12:35–46.
41. Fisher JLT-MR, Elliott J, Hards DK, Sims NA, Slavin J, Martin TJ, et al. Osteoprotegerin overexpression by breast cancer cells enhances orthotopic and osseous tumor growth and contrasts with that delivered therapeutically. Cancer Res 2006;66:3620–8.
42. Stein R, Gaillard S, McDonnell D. Estrogen-related receptor alpha induces the expression of vascular endothelial growth factor in breast cancer cells. J Steroid Biochem Mol Biol 2009;114:106–12.
43. Benslimane-Ahmim Z, Heymann D, Dizier B, Lokajczyk A, Brion R, Laurendeau I, et al. Osteoprotegerin, a new actor in vasculogenesis, stimulates endothelial colony-forming cells properties. J Thromb Haemost 2011;9:834–43.
44. Dwyer MAJJ, Wade HE, Eaton ML, Kunder RS, Kazmin D, Chang CY, et al. WNT11 expression is induced by estrogen-related receptor alpha and beta-catenin and acts in an autocrine manner to increase cancer cell migration. Cancer Res 2010;22:9298–308.
45. Lu XYC, Yuan M, Wei Y, Hu G, Kang Y. *In vivo* dynamics and distinct functions of hypoxia in primary tumor growth and organotropic metastasis of breast cancer. Cancer Res 2010;70:3905–14.
46. Fei JPF, Malaval L, Vico L, Lafage-Proust MH. Imaging and quantitative assessment of long bone vascularization in the adult rat using microcomputed tomography. Anat Rec (Hoboken) 2010;293:215–24.